Article

Chinese Science Bulletin

Astromechanics

December 2012 Vol.57 No.35: 4545–4551
doi: 10.1007/s11434-012-5484-5

Precise positioning of the Chang'E-3 lunar lander using a kinematic statistical method

HUANG Yong[1*], HU XiaoGong[1], LI PeiJia[1,2], CAO JianFeng[1,2,3], JIANG DongRong[1], ZHENG WeiMin[1] & FAN Min[4]

[1] *Shanghai Astronomical Observatory, Chinese Academy of Sciences, Shanghai 200030, China;*
[2] *Graduate University of Chinese Academy of Sciences, Beijing 100049, China;*
[3] *Beijing Aerospace Control and Command Center, Beijing 100094, China;*
[4] *Beijing Institute of Tracking and Telecommunications Technology, Beijing 100094, China*

Received February 28, 2012; accepted May 14, 2012

A kinematic statistical method is proposed to determine the position for Chang'E-3 (CE-3) lunar lander. This method uses both ranging and VLBI measurements to the lander for a continuous arc, combing with precise knowledge about the motion of the moon as provided by planetary ephemeris, to estimate the lander's position on the lunar surface with high accuracy. Accuracy analyses are carried out with simulation data using the software developed at Shanghai Astronomical Observatory in this study to show that measurement errors will dominate the position accuracy. Application of lunar digital elevation model (DEM) as constraints in the lander positioning is also analyzed. Simulations show that combing range/doppler and VLBI data, single epoch positioning accuracy is at several hundred meters level, but with ten minutes data accumulation positioning accuracy is able to be achieved with several meters. Analysis also shows that the information given by DEM can provide constraints in positioning, when DEM data reduce a 3-dimensional positioning problem to 2-dimensional. Considering the Sinus Iridum, CE-3 lander's planned landing area, has been observed with dedicated details during the CE-1 and CE-2 missions, and its regional DEM model accuracy may be higher than global models, which will certainly support CE-3's lander positioning.

lunar lander, positioning, lunar digital elevation model (DEM)

Citation: Huang Y, Hu X G, Li P J, et al. Precise positioning of the Chang'E-3 lunar lander using a kinematic statistical method. Chin Sci Bull, 2012, 57: 4545–4551, doi: 10.1007/s11434-012-5484-5

The first Chinese lunar explorer CE-1 was launched on October 24, 2007, and following CE-2 was launched on October 1, 2010 [1–3]. According to the long-term schedule, Chinese unmanned lunar exploration plan is divided into three stages: orbiting, landing and returning stages. In the orbiting stage, the CE-1 and CE-2 satellites fly around the moon and take photos about the landing area. In the landing stage, the main task is to softland on the lunar surface and to explore automatically [4]. A lunar lander and a rover are needed in this stage. How to determine the positions of the lander and rover on the lunar surface is very important to the following Chinese lunar exploration project. The rover moves very slowly and not far away from the lander, so the position determination of the lander is more critical.

Dealing with position determination of a satellite, the dynamic statistical orbit determination (OD) method and single point positioning are widely used in lunar exploration [1–3,5,6]. OD can be viewed as a special case of general parameter estimation problem, where the parameters characterizing the orbit of a satellite, have to be determined from observations using the least squares method. The main error sources are from observations as well as the force model, and in order to get high OD accuracy, forces exerting on the satellite must be modeled precisely. Comparing with dynamic OD method, single point positioning does not need to model forces, and the position of the satellite can be

*Corresponding author (email: yongh@shao.ac.cn)

determined geometrically. During orbital maneuver, soft-landing and surface walking, the dynamic OD method is not suitable for it is not easy to model precisely the forces exerted on the probe, while single point positioning can be used in these situations [3]. Generally, the accuracy of single point positioning is limited by the quality of observations and the geometry between ground stations and the satellite.

This paper studies how to determine the position of a lunar lander precisely, which is fixed and not moving on the lunar surface. A kinematic statistical method is proposed, which uses measurements of a continuous arc, combing with the motion of the moon, to get the position of the lander on the lunar surface with high accuracy. This statistical method uses all observations of a period, not a single point, to determine the position of a lunar lander, so the positioning accuracy is much higher than that of single point positioning.

The moon is 3.8×10^5 km far away from the earth averagely, so GDOP (geometry dilution of precision) for position determination of a lunar lander is much poor, which limits the position accuracy, especially using single point positioning. The statistical positioning method can get higher accuracy using more observations. In single point positioning, the interpolation of original observations is needed to get pseudo-observations corresponding to the same satellite time. While in kinematical statistical positioning method, the interpolation is not needed and positions at various epochs are connected by the motion of the lander, and all observations are used to create combined equations for solving parameters including the position of the lander with the least squares method. This method can also solve some other parameters such as range biases, and will work with only observations from single station.

There are similarities as well as significant differences between the kinematic statistical positioning for a lunar lander and the traditional OD for a satellite. Both use statistical method to get high accuracy. For the satellite, its motion around the center body is described with the forces exerting on the satellite, and the observations at various epochs are integrated via the state transfer matrix (STM) and processed simultaneously. Because the lander is fixed and not moving on the lunar surface, it is easy to establish the model of motion in inertial system, according to the motion of the moon. The model accuracy is only depended on the accuracy of lunar orbit and rotation.

With the development of lunar exploration, the accuracy of lunar digital elevation model (DEM) is improved dramatically. ULCN2005 (the unified lunar control network 2005) is the latest global control network of the moon, which has made use of historical photogrammetry measurements from Earth-based, Apollo, Marine 10, Galileo and Clementine missions. More than 3 million range measurements from the Chang'E-1 laser altimeter have been used to produce a global topographic model of the moon with improved accuracy, and a 360th degree and order spherical harmonic expansion of the lunar radii, is designated as Chang'E-1 lunar topography model s01 (CLTM-s01) [7]. A global lunar DEM with 3 km spatial resolution using the whole CE-1's laser altimeter (LAM) data was developed. The plane positioning accuracy is 445 m (1σ), and the vertical accuracy is 60 m (1σ) [8]. A global lunar topographic map with a spatial resolution of finer than 0.5 degree has been derived using data from the laser altimeter (LALT) on board the Japanese lunar explorer Selenological and Engineering Explorer (SELENE or Kaguya). A spherical harmonic model complete to degree and order 359 was developed, and the vertical accuracy is 77 m [9]. The altimetric data from the lunar orbiter laser altimeter (LOLA) in lunar reconnaissance orbiter (LRO) spacecraft have much higher accuracy, and the related DEM accuracy will be better than 10 m [10]. Considering the Sinus Iridum area, the future landing area for CE-3 probe, has been observed much more detailed in the CE-1 and CE-2 mission [11], and the regional DEM model accuracy may be higher than the global model.

The lunar DEM can be used in the calculation of the lander's position. The elevation information given by the DEM can serve as constraints, or the DEM can be directly used in the calculation, which reduces the 3-dimensional positioning problem to the 2-dimensional positioning. On the other hand, once the position of the lander is precisely determined, the results can also verify the accuracy of the DEM. The application of the lunar DEM in the position calculation is also studied in the paper.

1 Theory for the lander positioning

1.1 Motion of the lander

Considering the lander stands still on the moon, its equations of motion can be written in the moon-fixed coordinate system as $\begin{cases}\vec{r}(t)=\vec{r}_0,\\ \dot{\vec{r}}(t)=0,\end{cases}$ where $\vec{r}$ is the position of the lander, and it can be expressed as rectangular coordinate or geographic coordinate.

Estimated parameters which would not show up in the motion equation are defined as geometric parameters $\vec{p}_g$, including range bias and so on. The state vector can be defined as $X=\begin{pmatrix}\vec{r}\\ \vec{p}_g\end{pmatrix}$, then the equation of state is

$$\begin{cases}\dot{X}=0,\\ X(t_0)=X_0.\end{cases} \tag{1}$$

1.2 Equations of observations

The equation of the observation is the same as that in dynamic statistical OD. The state vector X_i corresponding to the observation Y_i can be indicated as

$$Y_i = G(X_i, t_i) + \varepsilon_i, \tag{2}$$

where X_i, Y_i, ε_i present the state vector, the observation and the noise at the epoch t_i respectively.

Since eq. (2) is nonlinear, linearization procedure should be conducted on the reference solution $X^*(t_i)$, and the equations are defined as

$$\begin{cases} y_i = Y_i - G(X_i^*, t_i), \\ \tilde{H}_i = \dfrac{\partial G}{\partial X}|_{X=X_i^*}, \\ H_i = \tilde{H}_i \Phi(t_i, t_0), \end{cases} \tag{3}$$

where $\Phi(t_i, t_0)$ is the state transition matrix, and for the positioning of the lander fixed on the lunar surface, it is the unit matrix.

Hence, the original nonlinear estimation problem can be replaced by the linear estimation problem described by

$$y_i = H_i x_0 + \varepsilon_i. \tag{4}$$

Define

$$y = \begin{pmatrix} y_1 \\ \vdots \\ y_k \end{pmatrix}, \quad H = \begin{pmatrix} H_1 \\ \vdots \\ H_k \end{pmatrix}, \quad \varepsilon = \begin{pmatrix} \varepsilon_1 \\ \vdots \\ \varepsilon_k \end{pmatrix}.$$

The equations for all observations can be written as

$$y = Hx_0 + \varepsilon. \tag{5}$$

The time and coordinate systems are inherent components of the OD program. For the positioning of the lander, the time system involves UTC (observation time), TAI, TDT and TDB, and the coordinate system involves the earth-centered and moon-centered references. The earth-centered reference includes the J2000.0 celestial reference and the earth-fixed reference, where precession, nutation and earth rotation are involved in the transformation between them. The moon-centered reference includes J2000.0 celestial reference and moon-fixed reference frame [1]. Furthermore, considering that the distance between the lander and the earth is far, it is necessary to build the observation model in the barycentric celestial reference, and the related coordinate time is TDB. The influence of general relativity should be considered [12].

During the foundation of the observation equations, the position of the lander in the inertial frame reference is adopted. However, the estimation state vector is in the moon-fixed frame reference. Due to that, the matrix H includes the transfer matrix between these two references.

Here $\vec{R}$ and $\vec{r}$ represent the position vector in the J2000.0 celestial reference and the moon-fixed reference respectively. The center body of the celestial frame reference here is the moon. Define the moon true-of-date system (TOD) as the intermediate reference system, the plane of which is the lunar equator with the X axis pointed to the cross point between the earth equator plane and lunar equator plane. The transformation of these two non-rotating systems involves two Euler angles (Ω' and is). The plane of the moon-fixed reference is the lunar equator with the X axis through the Sinus Medii on the lunar surface. To get moon-fixed reference, it can rotate the TOD system around the Z axis with angle Λ [1].

Ω', is and Λ are the three liberation angles of the moon. In the early 1900s, Hayn gave out the analytic functions for these three parameters, and later, koziel achieved the same formulas. However, the analytic expression appears in complex in the form with low accuracy [13,14]. Currently the three liberation angles are mainly obtained through the planet planetary ephemeris (such as JPL DE/LE403, 418, 421). The transformation between $\vec{R}$ and $\vec{r}$ is given as

$$\vec{r} = R_z(\Lambda) R_x(is) R_z(\Omega') \vec{R} = H_{gl} \vec{R}, \tag{6}$$

where R_x, R_y, R_z are rotations around the X, Y and Z axes, and H_{gl} is the conversion matrix between the two reference, and $H_{gl}^{-1} = H_{gl}^{\mathrm{T}}$. These three angles describe the lunar librations to a very high accuracy (2–3 cm accuracy for the lunar laser ranging) and were determined from numerically integrating the lunar orientation together with the planetary positions.

These three angles give a lunar body-fixed coordinate system with axes aligned with the lunar principal axes (PA). The lunar gravity field was developed using the lunar orientation specified by JPL planetary ephemeris. The IAU orientation is also a lunar body-fixed orientation with some lunar librations included but with the body-fixed axes specified by the mean-pole of the Moon (ME). These axes are offset from the principal axes of JPL planetary ephemeris by rotations using three small angles and amounts to about 1 km at the lunar surface for two of the angles. Coordinates in the PA system can be rotated to the ME system using the following expression (for DE421):

$$M = R_x(-0.30'') R_y(-78.56'') R_z(-67.92'') P, \tag{7}$$

where the angles are in seconds of arc and the rotations are around the body X, Y and Z axes. P and M are the position vectors of the PA system and ME system [15]. An ellipsoidal Moon with only a second-degree figure (gravity) would have the mean axis and principal axis frames coincident. Third- and higher-degree representations of the gravity field cause a constant rotation between the two frames. Our works are under the PA system.

1.3 Estimation method

Using batch algorithm with the least squares method, the best valuations of a certain epoch can be calculated with all observations. Because of the large amount observations and the statistical properties, the high precision result can be achieved. For satellite OD, high precision result of post processing usually uses the batch method.

According to the linear unbiased minimum variance estimation, value $\hat{x}_0$ is

$$\hat{x}_0 = (H^{\mathrm{T}}WH + \overline{P}_0)^{-1}(H^{\mathrm{T}}Wy + \overline{P}_0^{-1}\overline{x}_0), \tag{8}$$

where $\overline{x}_0$ and $\overline{P}_0$ are the priori values and the variance for the estimated parameters, and W is the weight matrix. The covariance matrix for vector $\hat{x}_0$ is

$$P_0 = (H^{\mathrm{T}}WH + \overline{P}_0)^{-1}. \tag{9}$$

Finally, the optimum estimation of $\hat{X}_0$ is

$$\hat{X}_0 = X^*{}_0 + \hat{x}_0. \tag{10}$$

2 Error analyses

During the process of dynamic statistical OD for the satellite, the main error sources are force errors and measurement errors. On contrast with the kinematic statistical positioning, the movement of the lunar lander is established using the lunar orbit and rotation, and thereby the main error sources affecting the positioning accuracy are measurement errors, which include the noise and the systematic bias, as well as errors of lunar orbit and rotation involved in the lunar ephemeris.

Nowadays the primary means to investigate lunar orbit and liberation is still the lunar laser ranging (LLR). The LLR observations are distances between the ground station and the reflector located on the lunar surface. From 1969 till now, the accuracy of LLR observations raised from 30 cm at the very beginning to 10–15 cm in the 1980s, and then 3–5 cm in the 1990s, until 2 cm in the nowadays. The primary purpose of LLR is to demonstrate the equivalence principle of Einstein's theory of relativity; however, with the development, LLR is used to determine the Earth orientation parameters (EOP), station coordinates, precession, nutation, parameters of lunar movements and liberation, coordinates of lunar surface reflectors and so on [16,17]. One of the scientific contributions of the LLR is that it significantly improved the accuracy of the lunar orbital motion, and contributed to the high-precision lunar ephemeris.

DE403 was built in 1995, and the updated series DE418 and DE421 ephemeris are using more LLR observations. For example, DE421 was using nearly 30 years LLR observations from 1970 to 2007, and achieving higher accuracy. The lunar position differences between DE418 and DE421 can reflect the model errors from a certain extent. Moreover, the lunar position difference in 2010 is up to 5 m between DE403 and other two ephemerides. However, it is about 0.5 m between DE418 and DE421. Therefore, JPL recommends the DE421 ephemeris in the following lunar exploration program [15].

The errors in lunar ephemeris and liberation models influence the lunar lander's poisoning accuracy directly. Based on the former analysis, the combined effects to the position calculation is about 1 m. Therefore, the main errors are from measurements, and this article focuses on analyzing the impact of measurement errors on the lander positioning.

3 Simulation results and analyses

Sinus Iridum (Latin for "bay of rainbows") is the future landing area for the CE-3 probe. It is a plain of basaltic lava that forms a northwestern extension to the Mare Imbrium. It is surrounded from the northeast to the southwest by the Montes Jura range. This bay and the surrounding mountains are considered one of the most beautiful features on the moon, and is a favorite among lunar observers. The selenographic coordinates of this bay are 44.1°N, 31.5°W, and the diameter is 259 km, with the area of 47750.927 km^2 [18].

Simulation data are applied to analyze the positioning accuracy of the lunar lander, using the software developed at Shanghai Astronomical Observatory (SHAO), Chinese Academy of Sciences. Assume that the lander is located at the center of Sinus Iridum, where selenographic coordinates are 44.1°N, 31.5°W. The elevation of the lander is −3338.0 m according to the ULCN2005 model.

Referring to tracking conditions of CE-1 and CE-2, simulation observations consist of Kashi and Jiamusi USB stations and the VLBI network consisting of 4 antennae located in Shanghai, Urumqi, Beijing and Kunming. Measurements noise errors (1σ) are 3 m, 2.5 mm/s, 3 ns, 1 ps/s for USB range, doppler, VLBI delay and delay rate, respectively. The data sampling rates are 1 s and 5 s for USB data and VLBI data respectively.

In calculation, the initial coordinates of the lander are 47.1°N, 34.5°W and −3000.0 m high, with the prior errors of 3 degree (about 100 km) on the lunar surface. Considering high accuracy of the lunar DEM and Sinus Iridum area is flat terrain [7–10], the initial elevation error is much smaller than the plane errors.

The position of the lunar lander is estimated using various tracking data combinations and various arc lengths. Table 1 shows the results, and the accuracies of the latitude and longitude in coordinates are expressed as distance errors on the lunar surface. Three strategies are adopted. Strategy 1 uses only range/doppler data of single station Jiamusi; Strategy 2 uses 2 station's range/doppler data; Strategy 3 adds VLBI data to strategy 1. All three strategies consider various arc lengths from several minutes to 1 hour.

From the results of Table 1, it can be concluded that using only USB data, the accuracy with 2 stations is much higher than that of single station, thus the capability of

Table 1 Position results of different strategies

Strategy	Arc length	Estimated position			Position errors		
		Lat. (°)	Long. (°)	Elev. (m)	Lat. (m)	Long. (m)	Elev. (m)
1	10 min	42.7288	–32.0434	–23690.7	–41592.9	–11838.0	–20352.7
	20 min	43.1436	–31.8798	–17731.6	–29010.7	–8273.8	–14393.6
	30 min	43.7663	–31.6329	–8466.6	–10122.9	–2894.8	–5128.6
	60 min	44.1654	–31.4783	–2251.9	1984.0	473.7	1086.1
2	10 min	44.1227	–31.4850	–3078.1	687.8	327.1	259.9
	20 min	44.0762	–31.5146	–3628.4	–721.2	–317.0	–290.4
	30 min	44.0802	–31.5120	–3581.2	–599.4	–261.1	–243.2
	60 min	44.0902	–31.5059	–3459.8	–297.3	–127.8	–121.8
3	Single epoch	44.1039	–31.5013	–3238.1	119.4	–27.3	99.9
	10 min	44.0998	–31.5000	–3340.6	–4.7	–1.0	–2.6
	20 min	44.0999	–31.5000	–3339.1	–1.6	0.1	–1.1

tracking the probe simultaneously for different stations is good for the lander positioning. The addition of VLBI observations improves the accuracy dramatically. The accuracy of 10 min positioning combined USB and VLBI data can reach 10 m, and even the accuracy of single epoch can reach several hundreds of meters.

Future analysis shows that according to the current accuracy of measurements, range data in USB and delay data in VLBI dominate the positioning result. There are range biases in the ranging measurements in CE-1/CE-2 mission, and the biases are stable and can be solved using long arc OD method. Assuming there are biases of 2 m left in range data, the analysis shows that the position accuracy does not decline much.

Figure 1 is the elevation graph of Sinus Iridum area using ULCN2005 model [7], and graphics scope is 39.2°–49.1°W, 36.4°–26.5°N. The lunar lander is at the center of the graph. From Figure 1 it is obvious that the topography of the central area of Sinus Iridum is flat and elevation changes no more than 400 m.

In calculation, the elevation information given by lunar DEM can be used as constraints. Considering the flat terrain in Sinus Iridum, elevations in the area do not change much. In Table 1, the elevation error in some situations is several kilometers, or even worse to dozens of kilometers, so the constraint in the elevation can be applied in the calculation to improve the accuracy of positioning and reduce the correlations between the parameters. In some situations, such as with seldom observations or rapid recovery, the prior elevation can be even fixed and only the latitude and longitude parameters are solved.

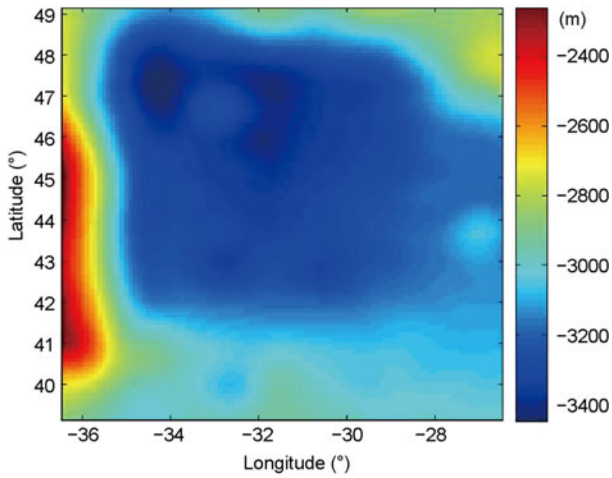

Figure 1 The elevation graph of Sinus Iridum area using ULCN2005 model.

In comparison with strategy 1, the elevation parameter is fixed and only other two parameters are solved. Table 2 shows the results, and the accuracy is much higher than the result of strategy 1. The positioning accuracy using 5–10 min USB data of single station can reach 1 km, and this approach can be used to meet rapid recovery requirements.

If the prior position error is much big, fringe searching technique can be used in the VLBI measuring [19], and VLBI delay rate data can be derived without delay data. Table 3 shows the results of combining USB data of single station Jiamusi and VLBI delay rate of 4 stations of single

Table 2 Position results with elevation parameter fixed using USB data of single station Jiamusi

Arc length	Estimated position			Position errors		
	Lat. (°)	Long. (°)	Elev. (m)	Lat. (m)	Long. (m)	Elev. (m)
5 min	44.1290	–31.4811	–3000.0	880.3	411.3	338.0
10 min	44.1245	–31.4875	–3000.0	742.0	272.0	338.0

Table 3 Results of combining USB data of single station Jiamusi and VLBI delay rate of single epoch

Strategy	Estimated parameters			Position errors		
	Lat. (°)	Long. (°)	Elev. (m)	Lat. (m)	Long. (m)	Elev. (m)
Fixing *H*	44.1471	−31.4557	−3000.0	1429.4	964.9	338.0
No fixing *H*	44.2314	−31.4382	−1431.6	3986.6	1346.5	1906.4

Table 4 Result of the method that DEM directly used in the calculation

Strategy 1	Estimated parameters			Position errors		
	Lat. (°)	Long. (°)	Elev. (m)	Lat. (m)	Long. (m)	Elev. (m)
5 min	44.1069	−31.4903	−3337.9	209.9	210.8	0.1

epoch, and approaches of fixing and not fixing the elevation parameter (H in the Table 3) are compared. The results show that the accuracy is about several kilometers, and then the motion model of the lander used in VLBI observing can be updated.

Besides as constraints, lunar DEM can also be directly used in the position calculation of the lunar lander, which reduces the 3-dimensional positioning to the 2-dimensional positioning. Still with strategy 1 of 5 min arc as an example, the positioning result of the method that DEM directly used in the calculation is showed in Table 4.

Though the elevation parameter accuracy using this method is very high in the simulation, the actual lunar DEM error is not considered in the simulation. Considering the lunar DEM error is about dozens of meters, and the spatial resolution is limited to several kilometers, the actual accuracy of the positioning of the lunar lander will be lower than that of simulation. However, in some situations that requiring rapid recovery of the lander's position, lunar DEM can be used to help improve the positioning accuracy. Sinus Iridum area has been observed much more detailed in the CE-1 and CE-2 mission, the regional DEM accuracy may be higher than the global model, and the regional DEM may be used in the future CE-3 mission.

4 Conclusions

This paper studies how to determine the position of a lunar lander precisely, which is fixed and not moving on the lunar surface. Considering the traditional dynamic OD method is not suitable and low accuracy with single point positioning method, a kinematic statistical method is proposed, and this method uses both ranging and VLBI measurements to the lander for a continuous arc, combing with precise knowledge about the motion of the moon as provided by planetary ephemeris, to estimate the lander's positions on the lunar surface with high accuracy.

This kinematic statistical method is used to analyze the position calculation of the lunar lander in Sinus Iridum area in future CE-3 mission. Simulations show that the accuracy of 10 min positioning combined USB and VLBI data can reach 10 m, and even the accuracy of single epoch can reach several hundreds of meters.

With the development of lunar DEM, the application of lunar DEM in position determination of the lunar lander is also discussed in the paper. Analysis shows the information given by DEM can provide constraints in positioning, and the DEM also can be directly used in the positioning, which reduces the 3-dimensional positioning to the 2-dimensional positioning. Position accuracy with elevation parameter fixed using USB data of single station of several minutes is better than 1 km, and this method can be used in some special situations. Considering the Sinus Iridum area has been observed much more detailed in the CE-1 and CE-2 mission, the regional DEM model accuracy is higher than the global model, which can be used in the future CE-3 mission.

The authors thank LI JinLing, HUANG ChengLi, PING JinSong, QIAN ZhiHang, LIU QingHui, ZHANG XiuZhong, WANG GuangLi, SHU FengChun and HONG XiaoYu for their comments and suggestions. This work was supported by the National Natural Science Foundation of China (11073047, 10703011) and Science and Technology Commission of Shanghai (12DZ2273300).

1 Huang Y. A study on the orbit determination of the Chang'E-1 lunar probe (in Chinese). Ph.D. Thesis. Shanghai: Shanghai Astronomical Observatory, Chinese Academy of Sciences, 2006
2 Chen M, Tang G S, Cao J F, et al. Precision orbit determination of CE-1 lunar satellite. Geomatics Inform Sci Wuhan Univ, 2011, 36: 212–217
3 Li J L, Liu L, Zheng W M, et al. The application of positioning reduction in the realtime stage of the Chang'E-2 project (in Chinese). Sci Sin Phys Mech Astron, 2011, 41: 889–895
4 Liu Q H, Chen M, Xiong W M, et al. Relative position determination of a lunar rover using high-accuracy multi-frequency same-beam VLBI. Sci China Phys Mech Astron, 2010, 53: 571–578
5 Yan J G, Ping J S, Li F, et al. Chang'E-1 precision orbit determination and lunar gravity field solution. Adv Space Res, 2010, 46: 50–57
6 Salzberg I M. Tracking the Apollo lunar rover with interferometry techniques. Proc IEEE, 1973, 61: 1233–1236
7 Ping J S, Huang Q, Yan J, et al. Lunar topographic model CLTM-s01 from Chang'E-1 laser altimeter. Sci China Ser G-Phys Mech Astron, 2009, 52: 1105–1114
8 Li C L, Ren X, Liu J J, et al. Laser altimetry data of Chang'E-1 and the global lunar DEM model. Sci China Earth Sci, 2010, 53: 1582–

1593
9 Araki H, Tazawa S, Noda H, et al. Lunar global shape and polar topography derived from Kaguya-LALT laser altimetry. Science, 2009, 323: 897–900
10 Mazarico E, Rowlands D D, Neumann G A, et al. Orbit determination of the lunar reconnaissance orbiter. J Geodesy, 2011, 85: 1066–1081
11 Li P J, Hu X G, Huang Y, et al. Orbit determination for Chang'E-2 lunar probe and evaluation of lunar gravity models. Sci China Phys Mech Astron, 2012, 55: 514–522
12 Cao J F, Huang Y, Hu X G, et al. Mars Express tracking and orbit determination trials with Chinese VLBI network. Chin Sci Bull, 2010, 55: 3654–3660
13 Zhang W, Liu L. The effects of physical libration of Moon on lunar satellites. Acta Astron Sin, 2005, 46: 196–206
14 Wang W R, Li F. Research and development of the lunar exploration. Prog Geophys, 2008, 23: 1751–1757
15 ftp://ssd.jpl.nasa.gov/pub/eph/planets/ioms/de421_moon_coord_iom.pdf
16 Zhen W M, Guo R, Li Y Q, et al. Research and experiment on the lunar laser ranging in China. Astron Res Tech, 2007, 4: 231–237
17 Huang C L, Jin W J, Xu H G. The terrestrial and lunar reference frame in LLR. Ann Shanghai Observ Acad Sin, 1996, 17: 169–175
18 Chen S B, Meng Z G, Cui T F, et al. Geologic investigation and mapping of the Sinus Iridum quadrangle from Clementine, SELENE, and Chang'E-1 data. Sci China Phys Mech Astron, 2010, 53: 2179–2187
19 Zhen W M, Shu F C, Zhang D. Application of software correlator to deep space VLBI tracking (in Chinese). J Astronaut, 2008, 29: 18–23